

Attenuation of Phosphorylation by Deoxycytidine Kinase is Key to Acquired Gemcitabine Resistance in a Pancreatic Cancer Cell Line: Targeted Proteomic and Metabolomic Analyses in PK9 Cells

Ken Ohmine · Kei Kawaguchi · Sumio Ohtsuki · Fuyuhiko Motoi · Shinichi Egawa · Michiaki Unno · Tetsuya Terasaki

Received: 4 November 2011 / Accepted: 29 February 2012 / Published online: 15 March 2012
© Springer Science+Business Media, LLC 2012

ABSTRACT

Purpose Multiple proteins are involved in activation and inactivation of 2',2'-difluorodeoxycytidine (gemcitabine, dFdC). We aimed to clarify the mechanism of dFdC resistance in a pancreatic cancer cell line by applying a combination of targeted proteomic and metabolomic analyses.

Methods Twenty-five enzyme and transporter proteins and 6 metabolites were quantified in sensitive and resistant pancreatic cancer cell lines, PK9 and RPK9, respectively.

Results The protein concentration of deoxycytidine kinase (dCK) in RPK9 cells was less than 0.02-fold (2%) compared with that in PK9 cells, whereas the differences (fold) were within a factor of 3 for other proteins. Targeted metabolomic analysis revealed that phosphorylated forms of dFdC were reduced to less than 0.2% in RPK9 cells. The extracellular concentration of 2',2'-difluorodeoxyuridine (dFdU), an inactive metabolite of dFdC, reached the same level as the initial dFdC concentration in RPK9 cells. However, tetrahydrouridine treatment did not increase phosphorylated forms of dFdC and did not reverse dFdC resistance in RPK9 cells, though this treatment inhibits production of dFdU.

Conclusions Combining targeted proteomics and metabolomics suggests that acquisition of resistance in RPK9 cells is due to attenuation of dFdC phosphorylation via suppression of dCK.

KEY WORDS drug resistance · gemcitabine · metabolomics · proteomics · pancreatic cancer

ABBREVIATIONS

ABC	ATP binding cassette
BCRP	breast cancer resistance protein
CDA	cytidine deaminase
CNT	concentrative nucleoside transporter
CTPS	cytidine 5'-triphosphate synthetase
dCK	deoxycytidine kinase
DCTD	deoxycytidylate deaminase
dFdC	2',2'-difluorodeoxycytidine or gemcitabine
dFdCDP	gemcitabine diphosphate
dFdCMP	gemcitabine monophosphate
dFdCTP	gemcitabine triphosphate
dFdU	2',2'-difluorodeoxyuridine
dFdUMP	2',2'-difluorodeoxyuridine monophosphate
ENT	equilibrative nucleoside transporter
Fara-AMP	9-beta-D-arabinofuranosyl-2-fluoroadenine monophosphate
LC-MS/MS	liquid chromatography-tandem mass spectrometer
MDR1	multidrug resistance protein 1
MRM	multiple reaction monitoring
MRP	multidrug resistance-associated proteins

Electronic supplementary material The online version of this article (doi:10.1007/s11095-012-0728-2) contains supplementary material, which is available to authorized users.

K. Ohmine · S. Ohtsuki · T. Terasaki (✉)
Division of Membrane Transport and Drug Targeting
Department of Biochemical Pharmacology and Therapeutics
Graduate School of Pharmaceutical Sciences, Tohoku University
6-3 Aoba, Aramaki, Aoba-ku
Sendai 980-8578, Japan
e-mail: terasaki.tetsuya@m.tohoku.ac.jp

K. Kawaguchi · F. Motoi · S. Egawa · M. Unno
Division of Hepato-Biliary Pancreatic Surgery
Department of Surgery
Graduate School of Medicine
Tohoku University
2-1 Seiryu-machi, Aoba-ku
Sendai 980-8574, Japan

5'-NT	cytosolic 5'-nucleotidase
RRM1	ribonucleotide reductase subunit 1
RRM2	ribonucleotide reductase subunit 2
THU	tetrahydrouridine

INTRODUCTION

Pancreatic cancer has an extremely poor prognosis, with a median survival time of only 8.6 months (1). 2',2'-Difluorodeoxycytidine (gemcitabine, dFdC) is currently the standard chemotherapeutic drug for metastatic and advanced pancreatic cancer, but affords only a modest improvement in survival (2–4). One of the reasons for the poor response to dFdC is thought to be acquired resistance (5).

Various proteins are considered to influence the anti-cancer effect of dFdC, as shown in Fig. 1. Equilibrative or concentrative nucleoside transporters are involved in transport of dFdC across the plasma membrane (6,7). dFdC is phosphorylated intracellularly via multiple steps, and the triphosphate (dFdCTP) inhibits DNA synthesis by interfering with incorporation of endogenous dCTP into DNA (8–10). The diphosphate (dFdCDP) is also an active metabolite, inhibiting ribonucleotide reductase; this results in a decrease

of intracellular dCTP, thereby suppressing DNA synthesis (11).

Given the multiplicity of proteins that may influence the anti-cancer effect of dFdC, it is not surprising that analyses of single proteins have yielded conflicting results. Equilibrative nucleoside transporter 1 (ENT1) plays a role in transport of dFdC into the cells, and higher expression of ENT1 was found to increase the sensitivity of cells to dFdC (12–14). Further, reduced expression of ENT1 gene was reported to correlate with shorter survival of pancreatic cancer patients (15). On the other hand, it was reported that resistant pancreatic cell lines expressed more ENT1 mRNA than sensitive cell lines, and suppression of ENT1 mRNA did not affect dFdC sensitivity in a pancreatic cancer cell line (16,17). The mRNA expression ratios of multiple molecules, including ENT1, deoxycytidine kinase (dCK) and ribonucleotide reductase, but not the individual expression levels, were found to be correlated with sensitivity to dFdC in several pancreatic cancer cells (18). These reports demonstrate the importance of systematic and comprehensive analysis to understand the mechanisms of dFdC resistance.

Evaluation of mRNA expression profile is one approach to the systematic analysis of anti-cancer resistance. However, mRNA expression does not always correlate with protein expression or function (19). Indeed, the mRNA level of dCK was reported not to correlate with the enzyme activity in leukocytes (20). Recently, however, it has become possible to quantify multiple proteins with high sensitivity using liquid chromatography-tandem mass spectrometer (LC-MS/MS) with multiple reaction monitoring (MRM) in combination with *in silico* selection of probe peptides (21). This method can measure changes in the expression of more than 30 proteins simultaneously. Therefore, we adopted this targeted approach to quantify the absolute amounts of various proteins considered to be potentially involved in dFdC resistance, in order to clarify changes in the protein network associated with drug resistance.

The activity of proteins is affected not only by protein expression levels, but also by activity per molecule. Variants in dCK or cytidine deaminase (CDA) have been reported to show decreased enzymatic activity and to modify cellular sensitivity to dFdC (22,23). Thus, it is also important to analyze metabolites. Since the distribution of each metabolite results from multiple processes, including uptake, efflux, phosphorylation and inactivation by transporters and enzymes, the combination approach to systematic analysis of target proteins and target metabolites shown in Fig. 1 is a rational strategy to identify proteins and processes that are involved in dFdC resistance.

Therefore, in the present study, our aim was to identify protein(s) and process(es) involved in acquisition of resistance to dFdC by comparing the amounts of multiple proteins and

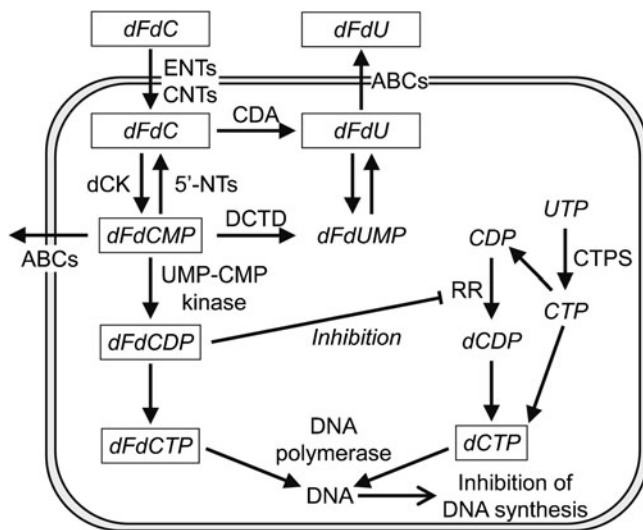


Fig. 1 Schematic illustration of transport and metabolism of dFdC. The indicated transporter and enzyme proteins, and compounds surrounded by a solid square were quantified by LC-MS/MS. As ATP binding cassette (ABC) transporters, multidrug resistance protein 1 (MDR1), multidrug resistance-associated proteins (MRPs) and breast cancer resistance protein (BCRP) were quantified. dFdCMP, dFdC monophosphate; dFdCDP, dFdC diphosphate; dFdCTP, dFdC triphosphate; dFdU, 2',2'-difluorodeoxyuridine; dFdUMP, dFdU monophosphate; ENT, equilibrative nucleoside transporter; CNT, concentrative nucleoside transporter; CDA, cytidine deaminase; dCK, deoxycytidine kinase; 5'-NT, cytosolic 5'-nucleotidase; DCTD, deoxycytidilate deaminase; RRM1, ribonucleotide reductase subunit 1; RRM2, ribonucleotide reductase subunit 2; CTPS, CTP synthetase.

metabolites in dFdC-sensitive and resistant pancreatic cancer cell lines, using quantitative targeted proteomics and quantitative targeted metabolomics.

MATERIALS AND METHODS

Reagents

dFdC was purchased from SynChem (Felsberg, Germany). 2',2'-Difluorodeoxyuridine (dFdU) and gemcitabine monophosphate (dFdCMP) were purchased from Toronto Research Chemicals (Ontario, Canada). dFdCDP and dFdCTP were purchased from JenaBioScience (Jena, Germany). Tetrahydrouridine (THU) was purchased from Calbiochem (Darmstadt, Germany). 9-beta-D-Arabinofuranosyl-2-fluoroadenine monophosphate (Fara-AMP) was purchased from LKT Labs (Saint Paul, MN, USA). DCK protein was purchased from Abcam (Cambridge, UK). All peptides listed in Tables S1 and S2 were purchased from Thermo Fisher Scientific (Sedatrabbe, Germany). All other reagents were commercial products of analytical grade.

Cell Culture and Subcellular Fractionation

Two human pancreatic adenocarcinoma cell lines, PK9 and RPK9, were established in the Division of Hepato-Biliary Pancreatic Surgery, Department of Surgery, Graduate School of Medicine, Tohoku University (Sendai, Japan). RPK9 was developed by continuously exposing PK9 cells to dFdC, with a starting concentration of 1 ng/ml (IC_{50} value of PK9), followed by stepwise increases to 1000 ng/ml. These cells were seeded onto non-coated tissue culture dishes (BD Biosciences Bedford, MA, USA) at the concentration of 1.5×10^4 cells/cm², and cultured in RPMI1640 (Invitrogen, Carlsbad, CA, USA) supplemented with 10% fetal bovine serum (FBS) (Moregate, Bulimba, Australia) at 37°C in a humidified atmosphere of 5% CO₂ in air. RPK9 cells retained more than 8×10^4 -fold resistance to dFdC, as compared with PK9 cells, and no change in the growth rate or shape of cells was observed during culture for more than 6 passages in medium without dFdC. The culture medium was exchanged every 2 days. PK9 and RPK9 cells in log growth phase were centrifuged and washed with phosphate-buffered saline (PBS). The pellet was suspended in a buffer of 50 mM Tris-HCl (pH 7.4), containing 500 μM phenylmethylsulfonyl fluoride (PMSF) and 2 mM dithiothreitol (DTT). The cells were placed in a chamber (Central Scientific Commerce, Tokyo, Japan) under a nitrogen pressure of 800 p.s.i., for 15 min at 4°C and cell lysis was performed by rapid decompression. After centrifugation at 100,000 g for 60 min at 4°C, the cell supernatant (cytosolic fraction) and precipitate (membrane fraction) were

used for quantification of enzyme and transporter proteins, and the cytosolic fraction was assayed for dFdC-phosphorylating, dFdCMP-dephosphorylating and dCK activities.

Quantification of Metabolites by MRM Analysis with LC-MS/MS

Cells were preincubated in drug-free medium for 24 h, then incubated with 1 μM dFdC or 1 μM dFdC and 500 μM THU for 10 min, or 1, 6, 12 or 24 h. The medium was centrifuged at 20,130 g for 5 min at 4°C. As an internal standard, 10 pmol of Fara-AMP in acetonitrile containing 2% formic acid was added to the supernatant. Cells were washed with PBS and lysed with 0.2 N NaOH. The lysate was neutralized with 1 N HCl, then 2% formic acid in acetonitrile containing 10 pmol of Fara-AMP was added. Each sample of medium and cell lysate was centrifuged at 20,130 g for 5 min at 4°C. The supernatant was dried under vacuum, resolubilized in 0.1% formic acid in water and analyzed by LC-MS/MS.

Sample analysis was automated by coupling a triple quadrupole mass spectrometer (QTRAP5500, AB Sciex, Foster City, CA, USA) to an Agilent 1200 high-performance liquid chromatography (HPLC) system (Agilent Technologies, Palo Alto, CA, USA). Briefly, 50 μl of each sample was injected onto a reversed-phase HPLC column (XDB-C18; 150 × 2.1 mm I. D.; particle size 5 μm; Agilent). Dihexylammonium acetate (DHAA) (Tokyo Chemical Industry, Tokyo, Japan) and ammonium formate were used to separate analytes; for conditions, see Tables S3 and S4. Peaks detected at non-target MRM transitions amounted to less than 3% of the peak of each authentic compound (10 pmol per injection) at the target MRM transition, taken as 100%, for all compounds. All compounds were quantified within the range of the calibration curves ($R^2 > 0.99$).

Quantification of Proteins by Multiplexed MRM Analysis with LC-MS/MS

The peptide probe for each protein was selected based on *in silico* criteria as described (21). The absolute amounts of proteins were determined by means of the multiplexed MRM method as described (21). The amino acid sequences and m/z values of the precursor ion and four product ions for each targeted protein are given in Tables S1 and S2. Prepared cytosolic and membrane fractions of cells were alkylated and digested with trypsin according to the reported method (21,24). The tryptic digests were acidified with formic acid and 100 fmol of isotope-labeled peptides was spiked into 100 μg of the digest to provide internal references, then the digests were analyzed by LC-MS/MS.

The sample analysis was automated by coupling a triple quadrupole mass spectrometer (QTRAP5500, AB Sciex) to

an Agilent 1200 HPLC system (Agilent Technologies). Each sample was injected onto a reversed-phase HPLC column (500×0.53 mm I.D., prepared in a fused silica capillary, provided by Shiseido); for conditions, see Table S5. Multiple products derived from single peptides were monitored at specific *m/z* transitions (Tables S1 and S2). Individual signal peaks were identified on the basis of equal retention times in each transition of multiple product ions.

Enzyme Activity

The reaction mixture (450 µl) for phosphorylating activity consisted of 50 mM Tris–HCl buffer (pH 7.4), 10 mM ATP, 10 mM MgCl₂, 10 mM NaF, 500 µM THU and 50 µM dFdC (for dFdC-phosphorylating activity) or 50 µM dCyd (for dCK activity). The reaction mixture (450 µl) for dFdCMP-dephosphorylating activity consisted of 50 mM Tris–HCl buffer (pH 7.0), 10 mM MgCl₂, 100 mM KCl, 5 mM DTT, 0.2 mg/ml BSA and 200 µM dFdCMP. Fifty µl of cytosolic fraction was added to the reaction mixture, and the final mixture was incubated at 37°C for 10 min, 1 h or 6 h. The reaction was stopped by the addition of cold 5% formic acid in acetonitrile containing 10 pmol of Fara-AMP as an internal standard (500 µl), and samples were centrifuged at 20,130 g for 5 min at 4°C. A 100 µl aliquot of the supernatant was dried under vacuum, and the residue was taken up in 0.1% formic acid in water and analyzed by LC-MS/MS.

Cytotoxicity Assay

The growth-inhibitory effect of dFdC on each cell line was assessed by means of colorimetric assay using a Cell Counting Kit (Dojindo, Kumamoto, Japan). Briefly, the cells were seeded on 96-well plates (1.6×10^4 cells/cm²) in culture medium containing 10% FBS. After 24 h, the cells were incubated with dFdC (0–3 mM) or with dFdC and 500 µM THU for 72 h, and then the cell viability was determined according to the manufacturer's instructions. Absorbance was measured at 450 nm with a microplate reader (Model 680, Bio-Rad Laboratories, Hercules, CA, USA). The IC₅₀ value was estimated by plotting cell viability *versus* drug concentration.

Reverse-Transcription Polymerase Chain Reaction (RT-PCR) Assay

RNA was isolated from PK9 and RPK9 cells by means of standard procedures using TRIZOL reagent (Invitrogen, Carlsbad, CA). Contaminating genomic DNA was digested with DNase I (Takara, Shiga, Japan), and cDNA was synthesized from 5 µg RNA in a volume of 12.5 µL with oligo-dT primer using ReverTra Ace (Toyobo, Osaka, Japan). Primers for PCR were as follows: dCK (forward 5'-TCTCTGAATGGCAAGCTCAA-3', reverse 5'-CTATG

CAGGAGCCAGCTTTC-3'), and β-actin (forward 5'-TTTGAGACCTTCAACCACCCC-3', reverse 5'-GTAGCTCTTCTCCAGGGAGG-3'). cDNA fragments were amplified under the following conditions: 94°C for 2 min, then 30 cycles of 98°C for 30 s, 58°C for 30 s, 72°C for 1 min. The PCR products were separated using 2.0% agarose gel electrophoresis and bands were visualized with an EPIPRO 7000 (Aisin, Aichi, Japan).

Data Analysis

The ion counts in the chromatograms were determined using the quantitation procedures in the Analyst software package version 1.5 (AB Sciex). dFdC metabolites were quantified by calculating the ratios of the peak areas to that of Fara-AMP (internal standard). To obtain the amounts of target proteins, the peptides were quantified by calculating the ratios of the peak areas to those of isotope-labeled peptides as described previously (21). All data are presented as the mean ± SEM.

RESULTS

Intracellular dFdC and Phosphorylated dFdC in PK9 and RPK9 Cells

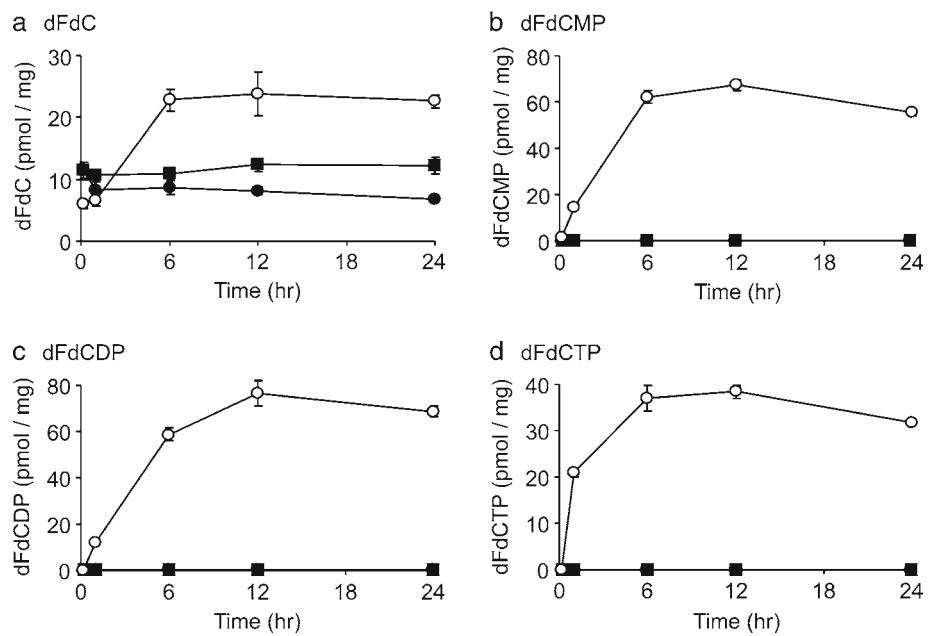
Pancreatic cancer cell line PK9 acquired dFdC resistance during exposure to dFdC. The IC₅₀ value of the resistant cell line, RPK9, was 2.8×10^5 -fold greater than that of PK9 cells. The amounts of dFdC and phosphorylated dFdC in cytosolic fraction of PK9 and RPK9 cells were compared after exposure to dFdC (Fig. 2). More than 10 pmol/mg protein of intracellular phosphorylated dFdC was detected in PK9 cells (Fig. 2b-d open circles), while in RPK9 cells, phosphorylated dFdC was below the detection limit (<0.1 pmol/mg protein) (Fig. 2b-d closed circles). This suggests that a decrease in phosphorylated dFdC metabolites was associated with dFdC resistance in RPK9 cells.

The amount of intracellular dFdC was also decreased to 30.1% in RPK9 cells compared to PK9 cells (Fig. 2a closed and open circles). The total amounts of intracellular dFdC and phosphorylated dFdC were decreased in RPK9 cells to less than about 4% of those in PK9 cells (under 8.41 pmol/mg protein and 206 pmol/mg protein after 12 h exposure).

Protein Levels of Enzymes and Transporters in PK9 and RPK9 Cells

The absolute protein concentrations of the transporters and enzymes shown in Fig. 1 were quantified and compared in the two cell lines (Tables I and II). The protein concentration of dCK in RPK9 cells was less than 0.02-fold compared with that in PK9 cells. The protein concentrations of CDA

Fig. 2 Intracellular levels of nucleoside metabolites of dFdC in PK9 and RPK9 cells. After incubation of PK9 cells (open circle) or RPK9 cells (closed circle) with dFdC, or RPK9 cells with dFdC and THU (closed square), intracellular levels of (a) dFdC, (b) dFdCMP, (c) dFdCDP and (d) dFdCTP were measured at 10 min, 1 h, 6 h, 12 h and 24 h incubation. Values are mean \pm SEM ($n=3$). dFdCMP, dFdCDP and dFdCTP in RPK9 cells were below the detection limit (0.1 pmol/mg protein).



and *de novo* enzymes, such as ribonucleotide reductase subunit 1 (RRM1), cytidine 5'-triphosphate synthetase 1 and 2 (CTPS1 and 2), were significantly greater in RPK9 cells. Among the transporters, the protein concentrations of ENT1 and multidrug resistance-associated proteins 1 and 4 (MRP1 and 4) in RPK9 were significantly greater than those in PK9 cells. There were no significant differences between the two cell lines in the protein concentrations of the other enzymes and transporters examined.

Uptake of dFdC into PK9 and RPK9 Cells

The amount of dFdC in the medium was determined to examine the involvement of ENT1 in the uptake of dFdC (Fig. 3). The amount of dFdC was not significantly different between the two cell lines after exposure to dFdC for 10 min to 12 h. More than 99% of initial dFdC was eliminated from the medium after 24 h in both cases.

Table 1 Protein Expression Levels of Enzymes in Cytosolic Fraction of PK9 and RPK9 Cells

Quantified protein	Protein concentration (fmol/ μ g protein)		Ratio of protein concentration between RPK9 and PK9 (fold)
	PK9	RPK9	
dCK	0.477 \pm 0.047	<0.01	<0.0210
UMP-CMP kinase	6.17 \pm 0.23	7.01 \pm 0.39	
CDA	0.276 \pm 0.018	0.454 \pm 0.032 **	1.64
DCTD	1.12 \pm 0.04	1.27 \pm 0.07	
cN-IA	<0.05	<0.05	
cN-IB	<0.05	<0.05	
cN-II	2.38 \pm 0.22	1.95 \pm 0.21	
cN-III	0.730 \pm 0.083	0.635 \pm 0.165	
RRM1	1.33 \pm 0.01	2.52 \pm 0.06 **	1.89
RRM2	<0.10	<0.10	
CTPS1	2.03 \pm 0.06	2.54 \pm 0.10 **	1.25
CTPS2	0.489 \pm 0.019	0.593 \pm 0.025 *	1.21

Cytosolic fraction from PK9 and RPK9 cells (50 μ g protein), spiked with 100 fmol of stable isotope-labeled peptide mixture, was injected into LC-MS/MS. The quantitative value (fmol/ μ g protein) was calculated from the peak area ratio of target and stable isotope-labeled peptide in each MRM transition. The amount of each enzyme was determined as the average from three or four MRM transitions with signal peaks. The protein amount of each enzyme in each sample is shown as mean \pm SEM ($n=3-4$). If the value was below the limit of quantification, the value of the quantification limit was used. ** $p < 0.01$ and * $p < 0.05$, significantly greater than the value in PK9 cells (Student's *t* test). The ratios of quantitative values in RPK9 to PK9 are shown on the right.

Table II Protein Expression Levels of Transporters in Membrane Fraction of PK9 and RPK9 Cells

Quantified protein	Protein concentration (fmol/ μ g protein)		Ratio of protein concentration between RPK9 and PK9 (fold)
	PK9	RPK9	
ENT1	1.92 \pm 0.08	2.59 \pm 0.06 **	1.35
ENT2	<2.00	<2.00	
CNT1	<0.20	<0.20	
CNT2	<0.20	<0.20	
CNT3	<0.20	<0.20	
MRP1	1.39 \pm 0.16	2.30 \pm 0.25 *	1.65
MRP2	0.504 \pm 0.115	0.561 \pm 0.060	
MRP3	<0.20	<0.20	
MRP4	0.508 \pm 0.055	1.14 \pm 0.05 **	2.24
MRP5	<2.00	<2.00	
MRP6	<0.20	<0.20	
MDR1	<0.20	<0.20	
BCRP	0.352 \pm 0.040	0.376 \pm 0.026	

Membrane fraction from PK9 and RPK9 cells (50 μ g protein), spiked with 100 fmol stable isotope-labeled peptide mixture, was injected into LC-MS/MS. The quantitative value (fmol/ μ g protein) was calculated from the peak area ratio of target and stable isotope-labeled peptides in each MRM transition. The amount of each transporter was determined as the average of three or four MRM transitions with signal peaks. The protein amount of each transporter in each sample is given as mean \pm SEM ($n=3-4$). If the value was below the limit of quantification, the value of the quantification limit was used. ** $p < 0.01$, * $p < 0.05$, significantly greater than quantitative value in PK9 cells (Student's t test). The ratios of quantitative values in RPK9 to PK9 are shown on the right.

Inactivation of dFdC by PK9 and RPK9 Cells

The amount of dFdU, one of the inactivated metabolites of dFdC, in the cells and medium was compared between PK9 and RPK9 cells, since total intracellular dFdC and phosphorylated dFdC were decreased in RPK9 cells. As shown in Fig. 4, in the case of RPK9 cells, extracellular dFdU was significantly increased, reaching a plateau at 1.63×10^3 pmol/well after 12 h; this is equal to the amount of dFdC initially present in the medium (1.63×10^3 pmol/well). In the case of PK9 cells, extracellular dFdU was equivalent to 35.9% of initial dFdC after 12 h. The amount of intracellular dFdU in RPK9 cells was smaller than that in PK9 cells. These results indicated that almost all dFdC was inactivated to dFdU and efficiently secreted into the medium by RPK9 cells.

Inhibition of Inactivating Enzyme for dFdC in RPK9 Cells

To clarify the contribution of induction of dFdC inactivation by CDA to the resistance, the effect of treatment with THU, a CDA inhibitor, was examined. THU treatment decreased the amount of dFdU in the medium of RPK9 cells to a level equivalent to 2% of initial dFdC (Fig. 4a), and intracellular dFdU was below the detection limit (<0.1 pmol/mg protein). Therefore,

THU treatment efficiently inhibited the inactivation of dFdC to dFdU.

THU treatment increased intracellular dFdC by 1.2–1.4 fold, but the intracellular levels of phosphorylated forms of dFdC in RPK9 cells were below the detection limit (<0.1 pmol/mg protein), as was the case in untreated cells (Fig. 2 closed squares and circles). As shown in Fig. 3, almost all of the initial dFdC remained intact in the medium at least up to 24 h in the presence of THU (Fig. 3 closed square). These results indicate that suppression of dFdC phosphorylation, but not induction of dFdC inactivation, is likely to be responsible for acquisition of resistance in RPK9 cells.

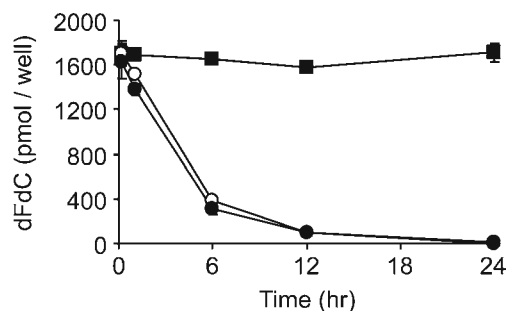


Fig. 3 Extracellular levels of dFdC in PK9 and RPK9 cells. After incubation of PK9 cells (open circle) or RPK9 cells (closed circle) with dFdC or RPK9 cells with dFdC in the presence of THU (closed square), extracellular levels of dFdC was measured at 10 min, 1 h, 6 h, 12 h and 24 h incubation. Values are mean \pm SEM ($n=3$).

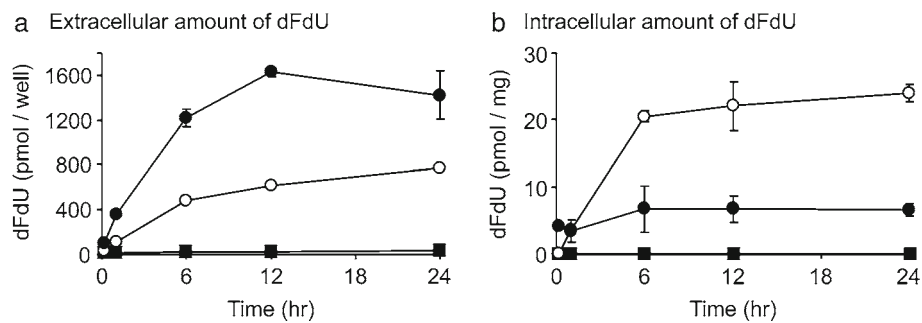


Fig. 4 Extracellular and intracellular levels of dFdU in PK9 and RPK9 cells. After incubation of PK9 cells (open circle) or RPK9 cells (closed circle) with dFdC or RPK9 cells with dFdC in the presence of THU (closed square), (a) extracellular and (b) intracellular levels of dFdU was measured at 10 min, 1 h, 6 h, 12 h and 24 h. Values are mean \pm SEM ($n=3$). Intracellular dFdU in RPK9 cells incubated with dFdC and THU was below the detection limit (0.1 pmol/mg protein).

Phosphorylation and Dephosphorylation of dFdC and its Monophosphate

Next, dFdC-phosphorylating activity and dFdCMP-dephosphorylating activity were examined using cell extract (25,26). As shown in Table III, dFdC-phosphorylating activity was decreased in RPK9 cells by more than 7.27-fold compared to PK9 cells. In contrast, dFdCMP-dephosphorylating activity was not significantly different in the two cell lines. Furthermore, phosphorylating activity towards dCyd, a specific substrate for dCK, was also analyzed to confirm that the decrease in dFdC phosphorylation in RPK9 cells was caused by suppression of dCK activity. The dCyd-phosphorylating activity in RPK9 cells was also decreased by more than 94.6%.

Suppression of dCK mRNA Expression in RPK9 Cells

mRNA expression of dCK were compared in PK9 and RPK9 cells by means of RT-PCR (Fig. 5). A band of the expected size for dCK (326 bp) was detected in the case of PK9 cells, whereas no such band was detected for RPK9 cells, indicating that dCK expression was greatly suppressed in RPK9 cells as

Table III Phosphorylation and Dephosphorylation Activities in PK9 and RPK9 Cells

Reaction	Enzyme activity (pmol/min/mg protein)	
	PK9	RPK9
Phosphorylation of dFdC to dFdCMP	1.01 \pm 0.05	<0.14
Dephosphorylation of dFdCMP to dFdC	523 \pm 19	672 \pm 54
Phosphorylation of dCyd to dCMP	9.20 \pm 2.00	<0.50

Enzyme activities represents mean \pm SEM ($n=3$). The amount of dFdCMP and dCMP, produced by phosphorylation of dFdC and dCyd, respectively, were below the detection limit in RPK9 cells. The lowest value in each calibration curve was taken as the detection limit

compared with PK9 cells in terms of mRNA, as well as protein expression and activity. The band intensity of β -actin was the same for PK9 and RPK9 cells, and no band was detected in the absence of reverse transcription.

Recovery of dFdC Phosphorylation upon Addition of dCK Protein

dCK protein was added to RPK9 cell extract to examine whether dCK could restore the dFdC-phosphorylating activity (Fig. 6). The amount of dFdCMP was below the limit of quantification in RPK9 cells when dCK was not added. When dCK protein purchased from Abcam (Cambridge, UK; ab99520) was added at the same concentration as in PK9 cells (0.477 fmol/ μ g protein, Table I), the amount of dFdCMP in RPK9 cells was increased to 385 ± 11 pmol/mg protein, which corresponds to 81.6% of that in PK9 cells.

Effect of CDA Inhibition by THU on dFdC Cytotoxicity

The effect of THU on the cytotoxicity of dFdC was examined (Table IV). In the absence of inhibitor, the IC_{50} value of dFdC for RPK9 cells was more than 1 mM, i.e., more than 2.8×10^5 -fold greater than that for PK9 cells (3.53 nM). In the presence of THU, the IC_{50} for RPK9 cells remained above 1 mM.

Production of dCTP by De Novo Enzymes in PK9 and RPK9 Cells

The amounts of intracellular dCTP in PK9 and RPK9 cells were compared to examine the influence of induction of *de novo* enzymes (Fig. 1). As shown in Table V the intracellular dCTP level was significantly increased in RPK9 cells by 2.09-fold compared with PK9 cells.

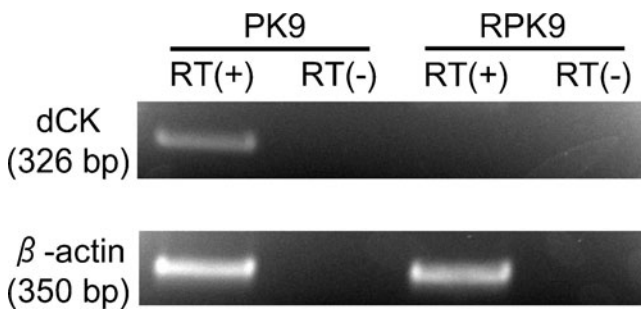


Fig. 5 mRNA expression of dCK in PK9 and RPK9 cells. Total RNA was isolated from the cells, reverse-transcribed and amplified (30 cycles) using primers for dCK and β -actin. Products were separated by gel electrophoresis and visualized. RT(+), with reverse transcription; RT(-), without reverse transcription (control).

DISCUSSION

The present study has established that the acquisition of dFdC resistance by RPK9 cells is due at least in part to attenuation of dFdC phosphorylation as a result of decreased expression of dCK; this was achieved by combining targeted proteomics and metabolomics, which offer higher sensitivity than global proteomics and metabolomics (27,28). In the present study, we were able to quantify 9 enzymes, 5 membrane transporters and 6 metabolites among those shown in Fig. 1, and compare their amounts in dFdC-sensitive and resistant cells. The changes in protein expression in RPK9 cells *versus* PK9 cells suggested four possible processes that might be involved in acquisition of dFdC resistance; i) attenuation of dFdC phosphorylation via suppression of dCK, ii) facilitation of dFdC inactivation to dFdU by induction of CDA, iii) facilitation of dCTP production by induction of ribonucleotide reductase

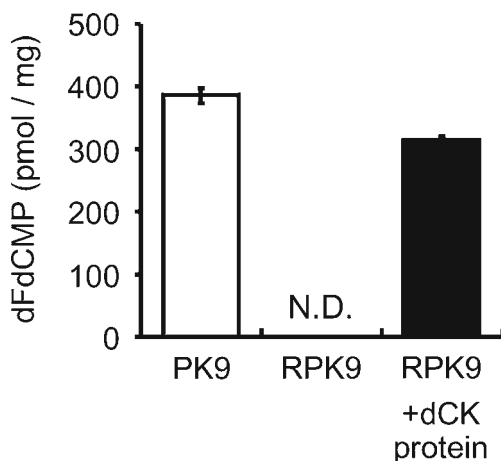


Fig. 6 Production of dFdCMP from dFdC in cell extracts of PK9 and RPK9. After incubation of cell extracts (20 μ g) of PK9 (open column) and RPK9 (closed column) with dFdC in the presence or absence of dCK protein (9.54 fmol) for 6 h, the amounts of dFdCMP were determined. Values are mean \pm SEM ($n=3$). N.D. means below the detection limit (<50 pmol/mg protein).

Table IV Comparison of IC_{50} Values of dFdC in PK9 and RPK9 Cells

Cell	Inhibitor	IC_{50} (nM)	Resistance ratio
PK9	–	3.53 ± 0.82	1
RPK9	–	$>1.0 \times 10^6$	$>2.8 \times 10^5$
	500 μ M THU	$>1.0 \times 10^6$	$>2.8 \times 10^5$

Growth inhibition was determined as described in Materials and Methods. The IC_{50} value in PK9 cells is the mean \pm SEM ($n=8$). Resistance ratio is the ratio of the IC_{50} value to that of the parental PK9 cell line

and CTPS, and iv) attenuation of dFdC uptake or facilitation of metabolite excretion by induction of ENT1 and/or MRPs. The most dramatic change was the decrease in dCK expression, and therefore attenuation of dFdC phosphorylation is likely to have been a key process for acquisition of resistance by RPK9 cells. However, we can not rule out a contribution of the other three processes.

The targeted metabolomic analysis showed that dFdC phosphorylation was strongly attenuated in RPK9 cells, and also showed almost all dFdC was converted to dFdU and excreted into the medium. While these processes involve many enzyme and transporter proteins, the attenuation of dFdC phosphorylation is consistent with dCK suppression, and the conversion to dFdU and excretion are consistent with induction of CDA, MRP4 and ENT1. Although it is not yet known whether dFdU is a substrate of MRP4 or ENT1, these results do show that the combination of targeted proteomics and metabolomics is a potent tool to identify altered processes and proteins in complex systems based on changes in protein expression and metabolite levels.

Treatment with THU did not restore the dFdC sensitivity of RPK9 cells, and did not increase intracellular levels of phosphorylated forms of dFdC (Fig. 2). THU treatment of RPK9 cell extract also did not increase dFdCMP level, whereas addition of dCK protein to RPK9 cell extract did increase the dFdCMP level (Fig. 6). Therefore, in RPK9 cells, CDA

Table V Intracellular Levels of dCTP in PK9 and RPK9 Cells in the Presence of dFdC

Time	Concentration of dCTP (pmol/mg protein)	
	PK9	RPK9
10 min	39.8 ± 3.7	75.2 ± 5.4 **
1 h	32.4 ± 2.9	68.1 ± 5.8 **
6 h	37.9 ± 1.8	65.4 ± 6.6 *
12 h	32.3 ± 3.3	64.2 ± 3.5 **
24 h	29.1 ± 1.1	60.9 ± 3.7 **

PK9 and RPK9 cells were incubated with dFdC, and the intracellular concentration of endogenous dCTP was measured by LC-MS/MS. Quantitative values (pmol/mg protein) are mean \pm SEM ($n=3$). ** $p < 0.01$ and * $p < 0.05$, significantly greater than in PK9 cells (Student's *t* test)

induction would not be a determinant of resistance acquisition, and conversion to dFdU was enhanced due to the lack of dFdC phosphorylation resulting from suppression of dCK expression (Tables I and III). Funamizu *et al.* demonstrated that treatment with THU increased the dFdC sensitivity of one pancreatic cancer cell line (BxPC-3), but did not affect the dFdC sensitivity of two other lines (Panc-1, MiaPaCa-2) (29). The present results raise the possibility that CDA inhibition did not increase phosphorylated forms of dFdC in Panc-1 and MiaPaCa-2 due to low dFdC phosphorylation activity, as was the case in RPK9 cells. In contrast, dCK mRNA expression in BxPC-3 cells was reported to be greater than in Panc-1 or MiaPaCa-2 cells, so BxPC-3 cells are expected to have high dFdC phosphorylation activity, and therefore CDA inhibition would increase the phosphorylated forms of dFdC.

ENT1 transports dFdC, and its protein expression was induced in RPK9 cells (6). Induction of ENT1 is expected to facilitate dFdC uptake, which would seem inconsistent with acquisition of resistance by RPK9 cells. Previous studies have yielded inconsistent results concerning the relation between ENT1 expression and acquisition of resistance (12–16). Elimination of dFdC from the medium was not changed in RPK9 cells, suggesting that intracellular metabolism, but not uptake from the medium, is the rate-limiting step for dFdC elimination. If this is so, the 1.35-fold induction of ENT1 would not have played a major role in acquisition of resistance by RPK9 cells. Nishio *et al.* reported that loss of localization of ENT2 in plasma membrane led to a decrease in uptake of dFdC and sensitivity in MiaPaCa2 cells (30). However, neither ENT2 nor ENT1 played a major role in acquisition of resistance by RPK9 cells, based on our findings on dFdC elimination from the medium. These results underline the importance of systematic analysis of multiple components to reliably identify key processes.

The protein expression level and activity of dCK were decreased by more than 98% and 90%, respectively, in RPK9 cells, and the decrease in the amount of phosphorylated dFdC in RPK9 cells was less than 0.3% when CDA was inhibited (Fig. 2, Tables I and III). dCK mRNA expression was also suppressed in RPK9 cells (Fig. 5). This good correlation among protein, activity and mRNA suppression in RPK9 supports the validity of protein quantification by means of the multiplexed-MRM method.

Kazuno *et al.* suggested that dCK activity was decreased by about 30% in pancreatic cancer cells with acquired resistance, MiaPaCa-2/dFdCyd, due to gene mutation, though there was no decrease in expression level (26). In RPK9 cells, the decrease in dCK activity might be explained by the decrease in protein expression, since the values of percent decrease were similar. However, the possibility of dCK gene mutation in RPK9 cells cannot be ruled out.

As a means to overcome dFdC resistance in RPK9 cells, exposure to dFdCMP might be expected to bypass the

suppression of dFdC phosphorylation in RPK9 cells. However, 53% of dFdCDP was converted to dFdC by dephosphorylation in the medium within 24 h at 37°C (data not shown), suggesting that dFdCMP in the medium might also be converted to dFdC. Also, the mechanism of dFdCMP uptake into the cells is unknown. On the other hand, induction of dCK activity might be an effective way to overcome dFdC resistance. Indeed, addition of dCK protein restored the conversion of dFdC to dFdCMP in RPK9 cell lysate (Fig. 6). Several of the enzymes and transporters that showed changes of protein expression in present targeted proteomic analysis, such as ENT1, MRP4, dCK, CDA and ribonucleotide reductase, have previously been suggested to play roles in acquisition of dFdC resistance (16,17,26,27,31–34). Therefore, it would not be surprising if different processes involving those proteins contribute to acquisition of dFdC resistance, depending on cell type or patients' background. The present results suggest that targeted proteomics can provide important expression information about related proteins to improve our understanding of complex processes of anti-cancer drug resistance. Furthermore, targeted proteomics by means of multiplexed-MRM can quantify targeted proteins with higher specificity than antibodies, since each target peptide is distinguished by mass information (m/z), and the peptide specificity can be confirmed by protein-database search. In addition, we found that a commercially available antibody against human dCK protein was not sufficiently sensitive to detect dCK protein in PK9 cells by western blotting (data not shown), though multiplexed-MRM could do so (Table I). This suggests the present targeted proteomics technology is sufficiently sensitive to quantify proteins related to dFdC resistance in cultured cells, and it may also be suitable for similar investigation of cancer tissues.

CONCLUSION

The present study serves as a model to show that mechanisms of nucleoside analog resistance can be clarified by targeted proteomic and metabolomic analyses using mass spectrometry, notwithstanding the great complexity of cellular pathways that may potentially be involved. Although we focused here on acquired resistance to gemcitabine in a single cell line, the present strategy should also be suitable for investigation of other cell lines and cancer tissues to clarify mechanisms of resistance to other anticancer drugs. It is also expected to aid the development of ways to overcome dFdC resistance, and to improve pancreatic cancer chemotherapy by allowing prediction of sensitivity to dFdC.

ACKNOWLEDGMENTS & DISCLOSURES

We thank K. Hamase for technical suggestions and Shiseido Co. Ltd for providing columns. This study was supported in

part by a Grant-in-Aid for JSPS Fellows, a Global COE Program from the Japan Society for the Promotion of Science, and a Grant for Development of Creative Technology Seeds Supporting Program for Creating University Ventures from Japan Science and Technology Agency. This study was also supported in part by the Industrial Technology Research Grant Program from the New Energy and the Industrial Technology Development Organization of Japan, and the Funding Program for Next Generation World-Leading Researchers by the Cabinet Office, Government of Japan.

REFERENCES

- Matsuno S, Egawa S, Fukuyama S, Motoi F, Sunamura M, Isaji S, Imaizumi T, Okada S, Kato H, Suda K, Nakao A, Hiraoka T, Hosotani R, Takeda K. Pancreatic Cancer Registry in Japan: 20 years of experience. *Pancreas*. 2004;28:219–30.
- Oettle H, Neuhaus P. Adjuvant therapy in pancreatic cancer. A critical appraisal. *Drugs*. 2007;67:2293–310.
- Carmichael J, Fink U, Russell RC, Spittle MF, Harris AL, Spiessi G, Blatter J. Phase II study of gemcitabine in patients with advanced pancreatic cancer. *Br J Cancer*. 1996;73:101–5.
- Li D, Xie K, Wolff R, Abbruzzese JL. Pancreatic cancer. *Lancet*. 2004;363:1049–57.
- Jordheim LP, Dumontet C. Review of recent studies on resistance to cytotoxic deoxynucleoside analogues. *Biochim Biophys Acta*. 2007;1776:138–59.
- Baldwin SA, Beal PR, Yao SY, King AE, Cass CE, Young JD. The equilibrative nucleoside transporter family, SLC29. *Pflugers Arch*. 2004;447:735–43.
- Gray JH, Owen RP, Giacomini KM. The concentrative nucleoside transporter family, SLC28. *Pflugers Arch*. 2004;447:728–34.
- Bouffard DY, Laliberte J, Momparler RL. Kinetic studies on 2',2'-difluorodeoxycytidine (Gemcitabine) with purified human deoxycytidine kinase and cytidine deaminase. *Biochem Pharmacol*. 1993;45:1857–61.
- Van Rompay AR, Johansson M, Karlsson A. Phosphorylation of deoxycytidine analog monophosphates by UMP-CMP kinase: molecular characterization of the human enzyme. *Mol Pharmacol*. 1999;56:562–9.
- Huang P, Chubb S, Hertel LW, Grindey GB, Plunkett W. Action of 2',2'-difluorodeoxycytidine on DNA synthesis. *Cancer Res*. 1991;51:6110–7.
- Heinemann V, Xu YZ, Chubb S, Sen A, Hertel LW, Grindey GB, Plunkett W. Inhibition of ribonucleotide reduction in CCRF-CEM cells by 2',2'-difluorodeoxycytidine. *Mol Pharmacol*. 1990;38:567–72.
- Marce S, Molina-Arcas M, Villamor N, Casado FJ, Campo E, Pastor-Anglada M, Colomer D. Expression of human equilibrative nucleoside transporter 1 (hENT1) and its correlation with gemcitabine uptake and cytotoxicity in mantle cell lymphoma. *Haematologica*. 2006;91:895–902.
- Achiwa H, Oguri T, Sato S, Maeda H, Niimi T, Ueda R. Determinants of sensitivity and resistance to gemcitabine: the roles of human equilibrative nucleoside transporter 1 and deoxycytidine kinase in non-small cell lung cancer. *Cancer Sci*. 2004;95:753–7.
- Lam W, Leung CH, Bussom S, Cheng YC. The impact of hypoxic treatment on the expression of phosphoglycerate kinase and the cytotoxicity of troxacitabine and gemcitabine. *Mol Pharmacol*. 2007;72:536–44.
- Giovannetti E, Del Tacca M, Mey V, Funel N, Nannizzi S, Ricci S, Orlandini C, Boggi U, Campani D, Del Chiaro M, Iannopollo M, Bevilacqua G, Mosca F, Danesi R. Transcription analysis of human equilibrative nucleoside transporter-1 predicts survival in pancreas cancer patients treated with gemcitabine. *Cancer Res*. 2006;66:3928–35.
- Tsuji M, Nakamori S, Nakahira S, Takahashi Y, Hayashi N, Okami J, Nagano H, Dono K, Umeshita K, Sakon M, Monden M. Human equilibrative nucleoside transporter 1, as a predictor of 5-fluorouracil resistance in human pancreatic cancer. *Anticancer Res*. 2007;27:2241–9.
- Ohhashi S, Ohuchida K, Mizumoto K, Fujita H, Egami T, Yu J, Toma H, Sadatomi S, Nagai E, Tanaka M. Down-regulation of deoxycytidine kinase enhances acquired resistance to gemcitabine in pancreatic cancer. *Anticancer Res*. 2008;28:2205–12.
- Nakano Y, Tanno S, Koizumi K, Nishikawa T, Nakamura K, Minoguchi M, Izawa T, Mizukami Y, Okumura T, Kohgo Y. Gemcitabine chemoresistance and molecular markers associated with gemcitabine transport and metabolism in human pancreatic cancer cells. *Br J Cancer*. 2007;96:457–63.
- Ohtsuki S, Schaefer O, Kawakami H, Inoue T, Liehner S, Sato A, Ishiguro N, Kishimoto W, Ludwig-Schwelling E, Ebner T, Terasaki T. Simultaneous absolute protein quantification of transporters, cytochrome P450s and UDP-glucuronosyltransferases as a novel approach for the characterization of individual human liver: Comparison with mRNA levels and activities. *Drug Metab Dispos*. 2011;40:83–92.
- Lotfi K, Karlsson K, Fyrberg A, Juliusson G, Jonsson V, Peterson C, Eriksson S, Albertioni F. The pattern of deoxycytidine- and deoxyguanosine kinase activity in relation to messenger RNA expression in blood cells from untreated patients with B-cell chronic lymphocytic leukemia. *Biochem Pharmacol*. 2006;71:882–90.
- Kamie J, Ohtsuki S, Iwase R, Ohmine K, Katsukura Y, Yanai K, Sekine Y, Uchida Y, Ito S, Terasaki T. Quantitative atlas of membrane transporter proteins: development and application of a highly sensitive simultaneous LC/MS/MS method combined with novel in-silico peptide selection criteria. *Pharm Res*. 2008;25:1469–83.
- Usova EV, Eriksson S. Identification of residues involved in the substrate specificity of human and murine dCK. *Biochem Pharmacol*. 2002;64:1559–67.
- Gilbert JA, Salavaggione OE, Ji Y, Pellemounter LL, Eckloff BW, Wieben ED, Ames MM, Weinshilboum RM. Gemcitabine pharmacogenomics: cytidine deaminase and deoxycytidylate deaminase gene resequencing and functional genomics. *Clin Cancer Res*. 2006;12:1794–803.
- Mawuenyega KG, Kaji H, Yamuchi Y, Shinkawa T, Saito H, Taoka M, Takahashi N, Isobe T. Large-scale identification of *Caenorhabditis elegans* proteins by multidimensional liquid chromatography-tandem mass spectrometry. *J Proteome Res*. 2003;2:23–35.
- Dumontet C, Fabianowska-Majewska K, Mantincic D, Callet Bauchu E, Tigaud I, Gandhi V, Lepoivre M, Peters GJ, Rolland MO, Wyczzechowska D, Fang X, Gazzo S, Voorn DA, Vanier-Viornery A, MacKey J. Common resistance mechanisms to deoxynucleoside analogues in variants of the human erythroleukaemic line K562. *Br J Haematol*. 1999;106:78–85.
- Kazuno H, Sakamoto K, Fujioka A, Fukushima M, Matsuda A, Sasaki T. Possible antitumor activity of 1-(3-C-ethynyl-beta-D-ribo-pentofuranosyl)cytosine (ECyd, TAS-106) against an established gemcitabine (dFdCyd)-resistant human pancreatic cancer cell line. *Cancer Sci*. 2005;96:295–302.
- Ohtsuki S, Uchida Y, Kubo Y, Terasaki T. Quantitative targeted absolute proteomics-based ADME research as a new path to drug discovery and development: Methodology, advantages, strategy, and prospects. *J Pharm Sci*. 2011;100:3547–59.

28. Barnidge DR, Dratz EA, Martin T, Bonilla LE, Moran LB, Lindall A. Absolute quantification of the G protein-coupled receptor rhodopsin by LC/MS/MS using proteolysis product peptides and synthetic peptide standards. *Anal Chem.* 2003;75:445–51.
29. Funamizu N, Okamoto A, Kamata Y, Misawa T, Uwagawa T, Gocho T, Yanaga K, Manome Y. Is the resistance of gemcitabine for pancreatic cancer settled only by overexpression of deoxycytidine kinase? *Oncol Rep.* 2010;23:471–5.
30. Nishio R, Tsuchiya H, Yasui T, Matsuura S, Kanki K, Kurimasa A, Hisatome I, Shiota G. Disrupted plasma membrane localization of equilibrative nucleoside transporter 2 in the chemoresistance of human pancreatic cells to gemcitabine (dFdCyd). *Cancer Sci.* 2011;102:622–9.
31. Reid G, Wielinga P, Zelcer N, De Haas M, Van Deemter L, Wijnholds J, Balzarini J, Borst P. Characterization of the transport of nucleoside analog drugs by the human multidrug resistance proteins MRP4 and MRP5. *Mol Pharmacol.* 2003;63:1094–103.
32. Bergman AM, Eijk PP, Ruiz van Haperen VW, Smid K, Veerman G, Hubeek I, van den Ijssel P, Ylstra B, Peters GJ. *In vivo* induction of resistance to gemcitabine results in increased expression of ribonucleotide reductase subunit M1 as the major determinant. *Cancer Res.* 2005;65:9510–6.
33. Goan YG, Zhou B, Hu E, Mi S, Yen Y. Overexpression of ribonucleotide reductase as a mechanism of resistance to 2,2-difluorodeoxycytidine in the human KB cancer cell line. *Cancer Res.* 1999;59:4204–7.
34. Ferrandina G, Mey V, Nannizzi S, Ricciardi S, Petrillo M, Ferlini C, Danesi R, Scambia G, Del Tacca M. Expression of nucleoside transporters, deoxycytidine kinase, ribonucleotide reductase regulatory subunits, and gemcitabine catabolic enzymes in primary ovarian cancer. *Cancer Chemother Pharmacol.* 2010;65:679–86.